Search for lepton flavour universality violation in $B^+ \to K^+\ell^+\ell^-$ decays

Paula Álvarez Cartelle

HEP seminar,
Imperial College London

June 26, 2019

The mighty Standard Model

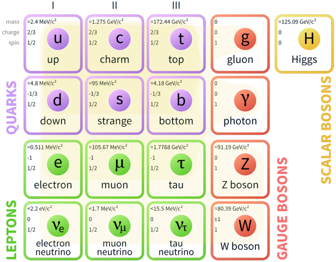

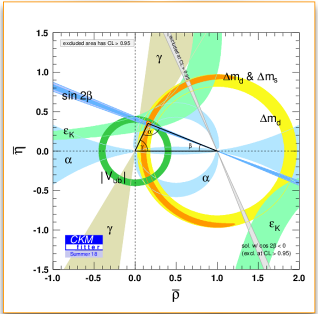

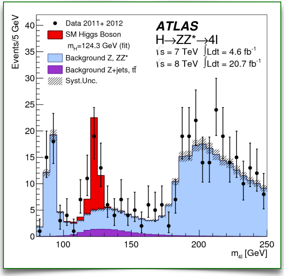

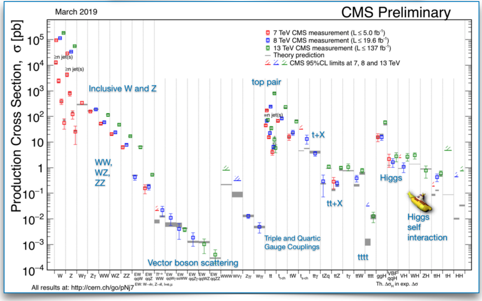

But...

- Still some open questions
  - Dark Matter
  - Nature of neutrino masses
  - Matter/Antimatter imbalance

- ... and also...
  - Why are there so many different fermions?
  - What is responsible for their organisation into generations/families?
  - Why are their masses/couplings so different?

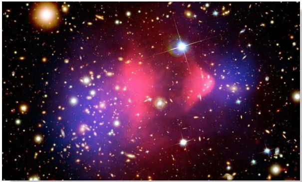

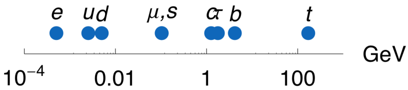

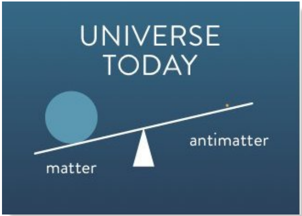

Quest for New Physics: The indirect approach

Direct search

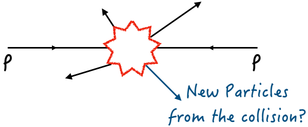

Indirect search

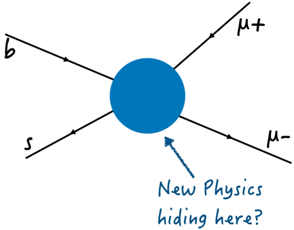

- Study processes that are suppressed or even forbidden in the SM - NP effects can then be relatively large
- Precision measurement of observables that are very well predicted in the SM
- Access to higher mass scales, due to virtual contributions, in a model independent way

Flavour Changing Neutral Currents

- FCNC transitions, such as $b \to s(d)l^+l^-$ decays, are excellent candidates for indirect NP searches

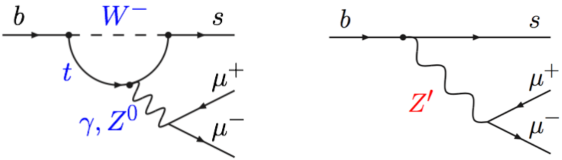

Strongly suppressed in the SM because

- arise only at the loop level
- quark-mixing is so hierarchical (off-diagonal CKM elements $\ll 1$)
- the GIM mechanism
- only the left-handed chirality participates in flavour-changing interactions

But these conditions **do not necessarily apply to physics beyond the SM!**

Exclusive decays

Unfortunately, we do not observe the quark-transition, but the hadron decay
$\Rightarrow$ We need to compute hadronic matrix elements (form-factors and decay constants)

$$b \to s\mu\mu \quad \Longrightarrow \quad B^+ \to K^+\mu^+\mu^-,\ B^0 \to K^{*0}\mu^+\mu^-,\ B_s \to \phi\mu^+\mu^- \ldots$$

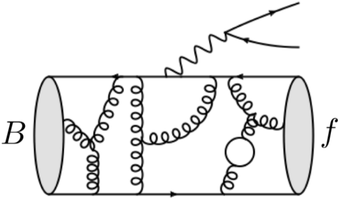

e.g. semileptonic decay

$\rightarrow$ Non-pertubative QCD, i.e. these are difficult to compute.

(Lattice QCD, QCD factorisation, Light-Cone sum rules...)

$\rightarrow$ Certain observables will profit from cancellation of these hadronic nuisances, making them more sensitive to New Physics contributions.

Flavour anomalies

In recent years, we have observed an interesting set of tensions with the SM predictions

A) **In $b \to s\ell^+\ell^-$ transitions (FCNC)**

- **Branching fractions** of $b \to s\mu^+\mu^-$ decays
- **Angular observables** in $b \to s\mu^+\mu^-$ decays
- **Lepton Flavour Universality tests** in μ/e ratios

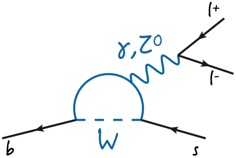

B) In $b \to c\ell\nu$ transitions (tree-level)

- Lepton Flavour Universality tests in μ/τ ratios

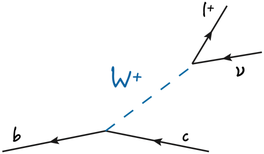

Branching fraction measurements

- Branching fractions consistently below the SM prediction at low $q^2 = [m(\ell^+\ell^-)]^2$ for many $b \to s\mu\mu$ processes

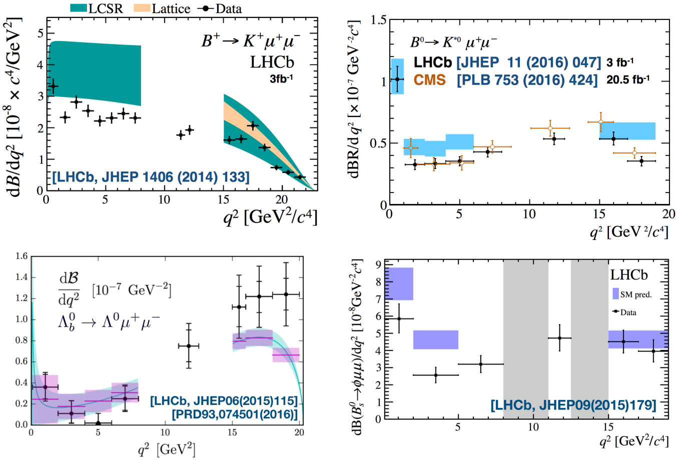

- SM predictions suffer from large hadronic uncertainties

Angular observables - $B^0 \to K^{*0}\mu^+\mu^-$ [LHCb, JHEP 02 (2016) 104]

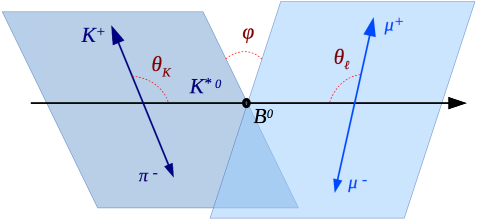

- Complementary constraints on NP & orthogonal experimental systematics compared to BR's
- Give access to observables with reduced dependence on hadronic effects [JHEP 1204 (2012) 104]

Angular observables - $B^0 \to K^{*0}\mu^+\mu^-$ [LHCb, JHEP 02 (2016) 104]

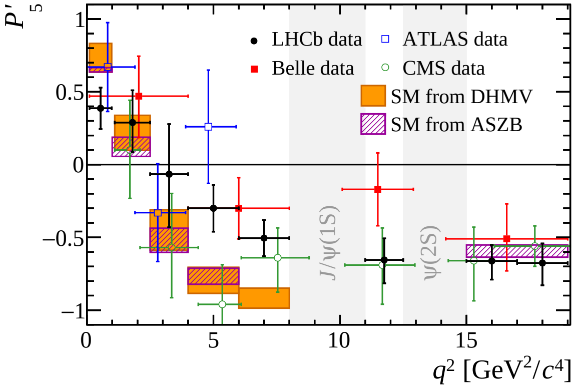

- Complementary constraints on NP & orthogonal experimental systematics compared to BR's
- Give access to observables with reduced dependence on hadronic effects [JHEP 1204 (2012) 104]

Theoretical framework - Effective theory

- Can describe these interactions in terms of an effective Hamiltonian that describes the full theory at lower energies (μ)

$$\mathcal{H}_{\text{eff}} \sim \sum_i C_i(\mu)\mathcal{O}_i(\mu)$$

$C_i(\mu) \rightarrow$ Wilson coefficient
(perturbative, short-distance physics, sensitive to $E > \mu$)

$\mathcal{O}_i \rightarrow$ Local operators
(non-perturbative, long-distance physics, sensitive to $E < \mu$)

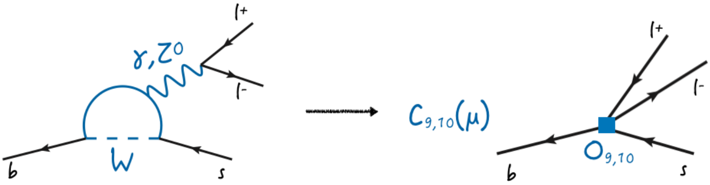

$\rightarrow$ Contributions from New Physics will modify the measured value of the Wilson coefficients present in the SM or introduce new operators

Global fits to $b \to s\mu^+\mu^-$ observables

[S. Descotes-Genon et al. JHEP06 (2016) 092]

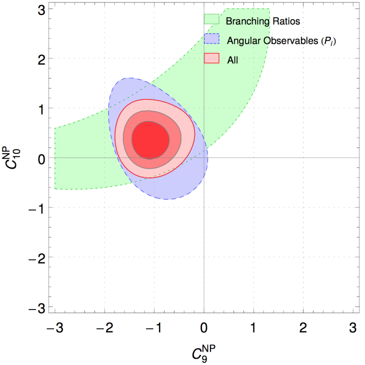

- Best fit prefers shifted vector coupling C_9 (or C_9 and axial-vector C_{10})
- Branching fractions and angular observables consistent

[W. Altmannshofer et al. Phys. Rev. D96 (2017) 055008,
B. Capdevila et al. JHEP 01 (2018) 093, T. Hurth et al. Phys. Rev. D96 (2017) 095034,
G. DAmico et al. JHEP 09 (2017) 010, L.-S. Geng et al. Phys. Rev. D96 (2017) 093006,
M. Ciuchini et al. Eur. Phys. J. C77 (2017) 688,
S. Jäger and J. Martin Camalich, Phys. Rev. D93 (2016) 014028 and many others]

New Physics or QCD?

Unaccounted for $c\bar{c}$-loop contributions would mimic vector-like NP $\Rightarrow$ shifts in C_9

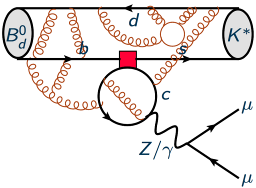

[Phys. Rev. D 98 (2018)]

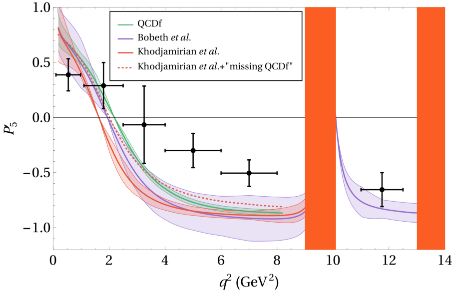

To resolve this situation:

- Improve experimental precision on angular observables
- Make new measurements of clean observables with reduced dependence on these theory uncertainties and still sensitive to NP effects...

Lepton flavour universality tests

- In the Standard Model, couplings of the gauge bosons to leptons are independent of lepton flavour
  $\rightarrow$ branching fractions of e, μ and τ differ only by phase space and helicity-suppressed contributions

- Ratios of the form:

$$R_K = \frac{BR(B^+ \to K^+ \mu^+ \mu^-)}{BR(B^+ \to K^+ e^+ e^-)} \overset{\text{SM}}{\cong} 1$$

$\rightarrow$ **Free from QCD uncertainties that may affect other observables**
(hadronic effects cancel in the ratio, error is $\mathcal{O}(10^{-4})$ [JHEP 07 (2007) 040])

$\rightarrow$ QED corrections can be $\mathcal{O}(10^{-2})$ [EPJC 76 (2016) 8,440]

- Any sign of lepton flavour non-universality would be a direct sign for New Physics

R_K & R_{K^*} with LHCb Run 1

[LHCb, PRL 113 (2014) 151601]
[LHCb, JHEP 08 (2017) 055]
[BaBar, PRD 86 (2012) 032012]
[Belle, PRL 103 (2009) 171801]

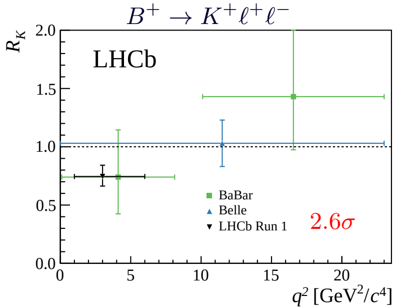

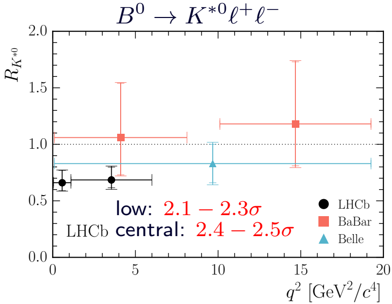

- Both results below the SM expectation, although significance is still low.
- Tensions could be explained, together with anomalous measurements in $b \to s\mu\mu$ decays, in a coherent NP picture.

R_K & R_{K^*} with LHCb Run 1

[LHCb, PRL 113 (2014) 151601]
[LHCb, JHEP 08 (2017) 055]
[BaBar, PRD 86 (2012) 032012]
[Belle, PRL 103 (2009) 171801]

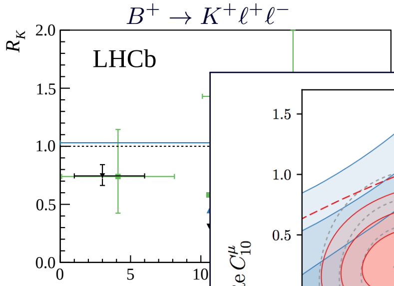

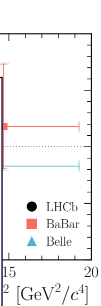

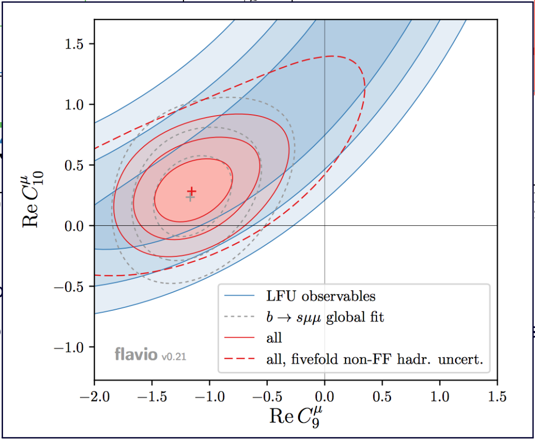

- Both results belo … low.
- Tensions could b … s in $b \to s\mu\mu$ decays,

[W. Altmannshofer et al., PRD 96 (2017) 055008]

The LHCb detector

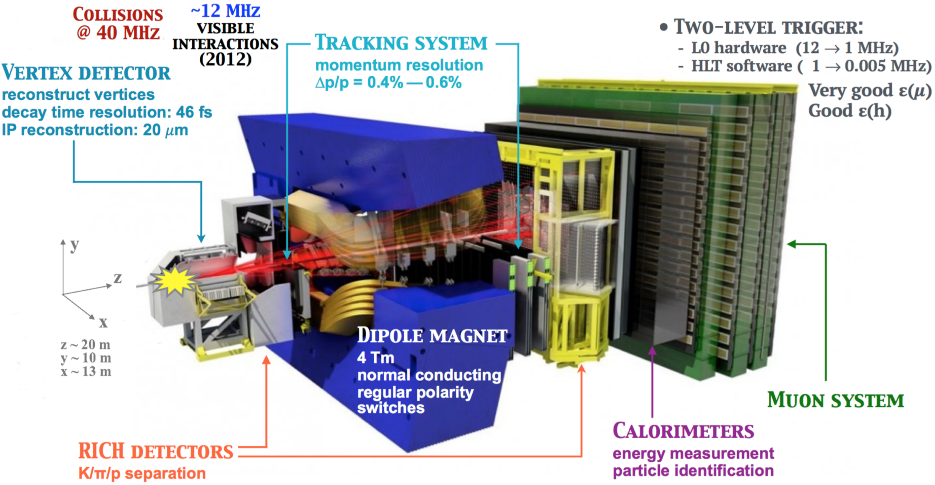

LFU in $B^+ \to K^+\ell^+\ell^-$

$$R_K = \frac{\int_{1.1\ \mathrm{GeV}^2}^{6.0\,\mathrm{GeV}^2} \frac{\mathrm{d}\mathcal{B}(B^+\to K^+\mu^+\mu^-)}{\mathrm{d}q^2}\mathrm{d}q^2}{\int_{1.1\,\mathrm{GeV}^2}^{6.0\,\mathrm{GeV}^2} \frac{\mathrm{d}\mathcal{B}(B^+\to K^+e^+e^-)}{\mathrm{d}q^2}\mathrm{d}q^2}$$

Measurement performed in $\mathbf{1.1 < q^2 < 6.0\,GeV^2/c^4}$ on

- Reanalysed **2011 & 2012 data (3 fb^{-1})**,

  $\rightarrow$ Improved reconstruction and re-optimised analysis strategy

- Added **2015 and 2016 datasets (∼2 fb^{-1})**,

  $\rightarrow$ Larger $b\bar{b}$ cross-section due to higher $\sqrt{s}$

In total, this update uses **∼twice as many B's as previous analysis**.

Electron Bremsstrahlung

Electrons lose a large fraction of their energy through Bremsstrahlung radiation

Bremsstrahlung recovery procedure to improve momentum measurement for electrons
$\rightarrow$ Look for photon clusters in the calorimeter ($E_T > 75\,\mathrm{MeV}$) compatible with electron direction before magnet

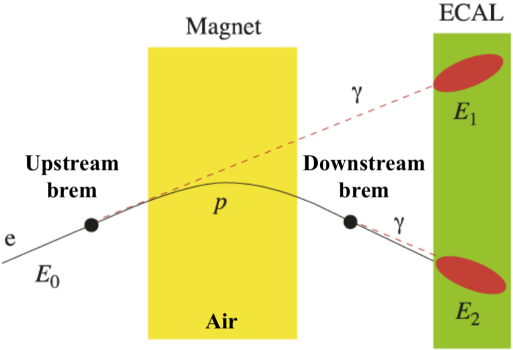

Electrons VS Muons

[PRL 122 (2019) 191801]

1. Even after Bremsstrahlung recovery, electrons still have degraded momentum, and mass/q^2 resolution

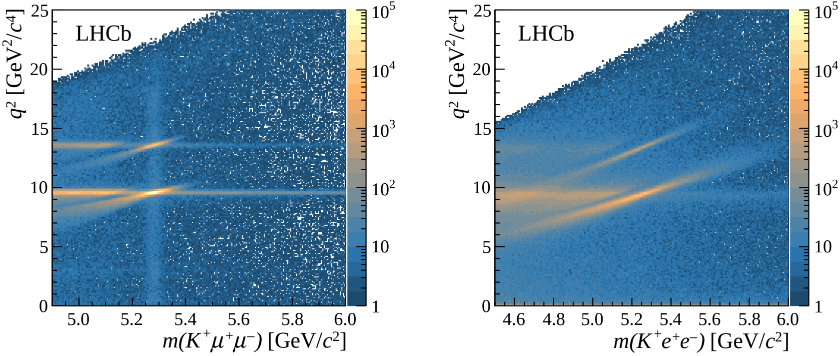

Electrons VS Muons

[PRL 122 (2019) 191801]

1. Even after Bremsstrahlung recovery, electrons still have degraded momentum, and mass/q^2 resolution

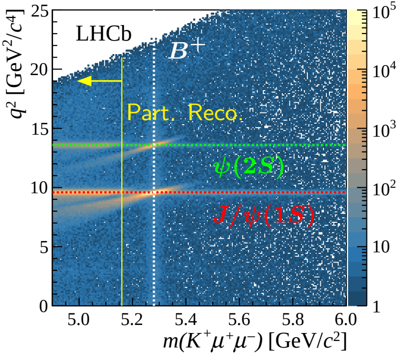

Electrons VS Muons

1. Even after Bremsstrahlung recovery, electrons still have degraded momentum, and mass/q^2 resolution
2. Very different trigger signatures: Lower trigger efficiency for electrons
   - Muons identified by Muon stations
   - Electrons rely on signal in the Calorimeter (higher occupancy $\Rightarrow$ higher trigger thresholds)

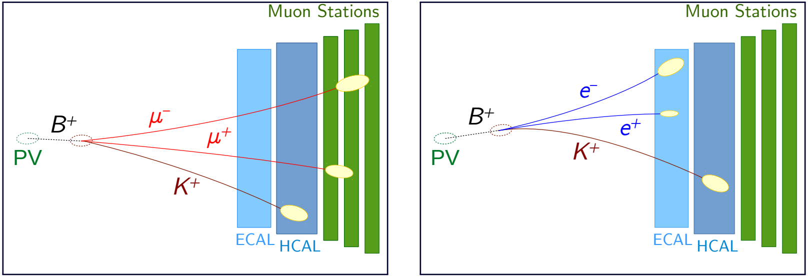

Electrons VS Muons

1. Even after Bremsstrahlung recovery, electrons still have degraded momentum, and mass/q^2 resolution
2. Very different trigger signatures: Lower trigger efficiency for electrons
   - Muons identified by Muon stations
   - Electrons rely on signal in the Calorimeter (higher occupancy $\Rightarrow$ higher trigger thresholds)

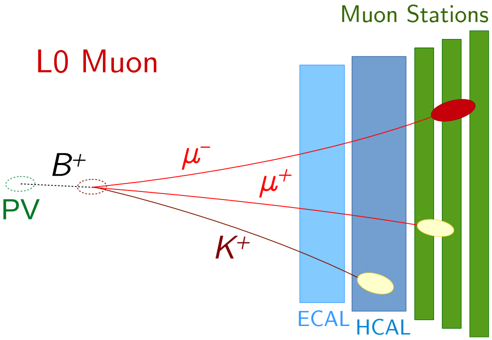

Electrons VS Muons

1. Even after Bremsstrahlung recovery, electrons still have degraded momentum, and mass/q^2 resolution
2. Very different trigger signatures: Lower trigger efficiency for electrons
   - Muons identified by Muon stations
   - Electrons rely on signal in the Calorimeter (higher occupancy $\Rightarrow$ higher trigger thresholds)

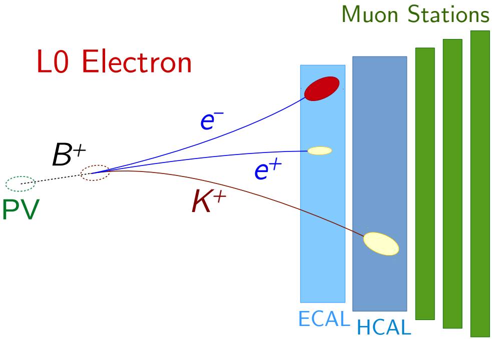

Electrons VS Muons

1. Even after Bremsstrahlung recovery, electrons still have degraded momentum, and mass/q^2 resolution
2. Very different trigger signatures: Lower trigger efficiency for electrons
   - Muons identified by Muon stations
   - Electrons rely on signal in the Calorimeter (higher occupancy $\Rightarrow$ higher trigger thresholds)

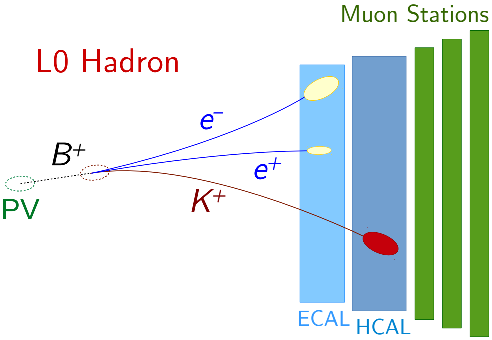

Electrons VS Muons

1. Even after Bremsstrahlung recovery, electrons still have degraded momentum, and mass/q^2 resolution
2. Very different trigger signatures: Lower trigger efficiency for electrons
   - Muons identified by Muon stations
   - Electrons rely on signal in the Calorimeter (higher occupancy $\Rightarrow$ higher trigger thresholds)

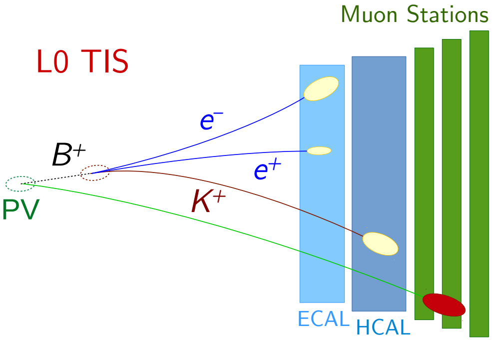

Electrons VS Muons

1. Even after Bremsstrahlung recovery, electrons still have degraded momentum, and mass/q^2 resolution
2. Very different trigger signatures: Lower trigger efficiency for electrons
   - Muons identified by Muon stations
   - Electrons rely on signal in the Calorimeter (higher occupancy $\Rightarrow$ higher trigger thresholds)
3. Particle ID and track reconstruction efficiencies also larger for muons than for electrons

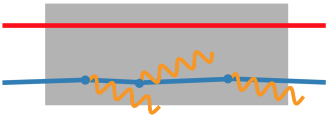

Electrons VS Muons

1. Even after Bremsstrahlung recovery, electrons still have degraded momentum, and mass/q^2 resolution
2. Very different trigger signatures: Lower trigger efficiency for electrons
   - Muons identified by Muon stations
   - Electrons rely on signal in the Calorimeter (higher occupancy $\Rightarrow$ higher trigger thresholds)
3. Particle ID and track reconstruction efficiencies also larger for muons than for electrons

$\rightarrow$ **Critical aspect of the analysis: Get the differences between electron and muon efficiencies fully under control**

Strategy

$$R_K = \frac{\mathcal{B}(B^+ \to K^+ \mu^+ \mu^-)}{\mathcal{B}(B^+ \to K^+ J/\psi(\mu^+ \mu^-))} \Bigg/ \frac{\mathcal{B}(B^+ \to K^+ e^+ e^-)}{\mathcal{B}(B^+ \to K^+ J/\psi(e^+ e^-))}$$

$$= \quad \frac{N(B^+ \to K^+ \mu^+ \mu^-)}{N(B^+ \to K^+ J/\psi(\mu^+ \mu^-))} \times \frac{\varepsilon_{B^+ \to K^+ J/\psi(\mu^+ \mu^-)}}{\varepsilon_{B^+ \to K^+ \mu^+ \mu^-}}$$

$$\times \frac{N(B^+ \to K^+ J/\psi(e^+ e^-))}{N(B^+ \to K^+ e^+ e^-)} \times \frac{\varepsilon_{B^+ \to K^+ e^+ e^-}}{\varepsilon_{B^+ \to K^+ J/\psi(e^+ e^-)}}$$

- R_K is measured as a **double ratio** to cancel out most systematics

  $\rightarrow$ $B^+ \to K^+ J/\psi(\ell^+ \ell^-)$ measured to be LF-universal within 0.4%

- Yields determined from a fit to the invariant mass of the final state particles

- Efficiencies computed using simulation that is calibrated with control channels in data

Strategy (II)

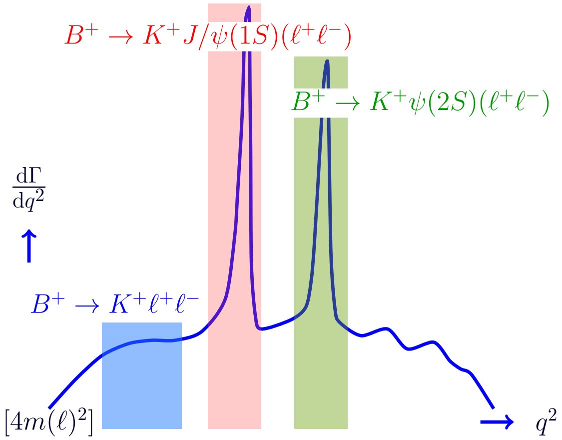

Resonant and nonresonant are separated in q^2

$\to$ However, good overlap between $B^+ \to K^+\ell^+\ell^-$ and $B^+ \to K^+ J/\psi(\ell^+\ell^-)$ in the variables relevant to the detector response

Selection & backgrounds

[PRL 122 (2019) 191801]

- Identical selection between resonant and rare modes (except for q^2 and $m(K^+\ell^+\ell^-)$ requirements)
- Use particle ID requirements and mass vetoes to suppress peaking backgrounds from exclusive B-decays to negligible levels
  - Backgrounds from $b \to c \to s$ cascade decays
  - Mis-ID backgrounds, e.g. $B \to K\pi^+_{(\to e^+)}\pi^-_{(\to e^-)}$
- Multivariate selection to reduce combinatorial background and improve signal significance (BDT)

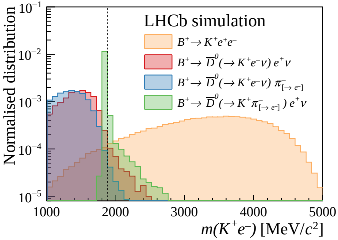

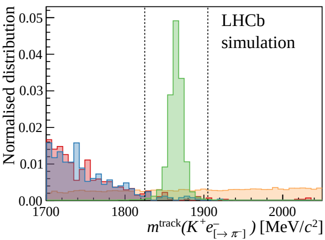

Efficiency calibration

Ratio of efficiencies determined with simulation carefully calibrated using control channels selected from data:

- Particle ID calibration
  - Tune particle ID variables for diff. particle species using kinematically selected calibration samples ($D^{*+} \to D^0(K^-\pi^+)\pi^+ ...$) [EPJ T&I(2019)6:1]
- Calibration of q^2 and $m(K^+e^+e^-)$ resolutions
  - Use fit to $m(J/\psi)$ to smear q^2 in simulation to match that in data
- Calibration of B^+ kinematics
- Trigger efficiency calibration

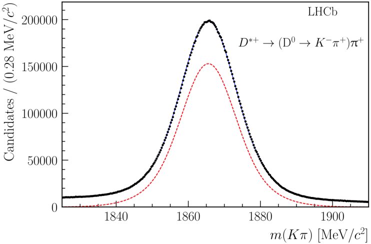

Calibration of B^+ kinematics

[PRL 122 (2019) 191801]

- Calibrate the simulation so that it describes correctly the kinematics of the B^+'s produced at LHCb.
- Compare distributions in data and simulation using $B^+ \to K^+ J/\psi(\ell^+\ell^-)$ candidates.
- Iterative reweighing of $p_T(B^+) \times \eta(B^+)$, but also the vertex quality and the significance of the B^+ displacement.

none

$\mu\mu$ `L0Muon, nominal`

$\mu\mu$ `L0TIS`

ee `L0Electron`

$VTX\chi^2$: ee `L0Electron`, $p_T(B){\times}\eta(B)$, $IP\chi^2$: $\mu\mu$ `L0Muon`

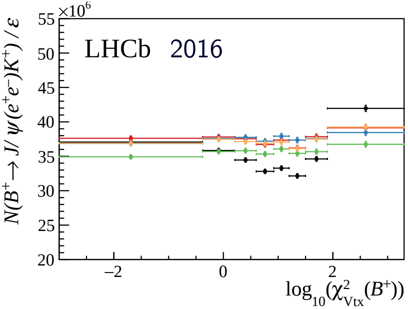

$\to$ Systematic uncertainty from RMS between all these weights

Trigger efficiency

[PRL 122 (2019) 191801]

The trigger efficiency is computed in data using $B^+ \to K^+ J/\psi(\ell^+\ell^-)$ decays through a tag-and-probe method

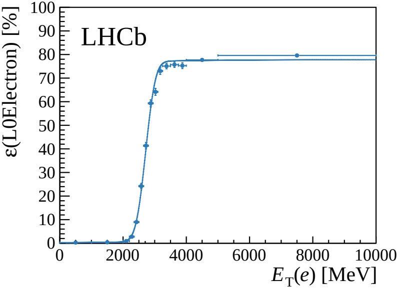

Especially for the electron samples, need to take into consideration some subtleties:

- dependence on how the calibration sample is selected,
- correlation between the two leptons in the signal.

Repeat calibration with different samples/different requirements on the accompanying lepton

$\rightarrow$ Associated systematic in the ratio of efficiencies is small

$$\varepsilon_{B^+\to K^+\ell^+\ell^-} / \varepsilon_{B^+\to K^+ J/\psi(\ell^+\ell^-)}$$

Efficiency calibration summary

[PRL 122 (2019) 191801]

- After calibration, very good data/MC agreement in all key observables

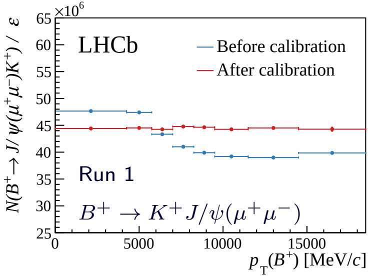

Cross-check 1: Measurement of $r_{J/\psi}$ [PRL 122 (2019) 191801]

- To ensure that the efficiencies are under control, check

$$r_{J/\psi} = \frac{\mathcal{B}(B^+ \to K^+ J/\psi(\mu^+\mu^-))}{\mathcal{B}(B^+ \to K^+ J/\psi(e^+e^-))} = 1,$$

  known to be true within 0.4%.

- Very stringent check, as it requires direct control of muons vs electrons.

- Result:

$$r_{J/\psi} = 1.014 \pm 0.035\ (\mathrm{stat} + \mathrm{syst})$$

- Checked that the value of $r_{J/\psi}$ is compatible with unity for both Run 1 and Run 2 datasets, and in all trigger samples.

Cross-check 2: $r_{J/\psi}$ as a function of kinematics

Check that efficiencies are understood in all kinematic regions $\rightarrow$ $r_{J/\psi}$ is flat for all variables examined

$\rightarrow$ e.g. given expected $\min(p_T(\ell^+), p_T(\ell^-))$ spectra, bias expected on R_K if deviations are genuine rather than fluctuations is 0.1%

[PRL 122 (2019) 191801]

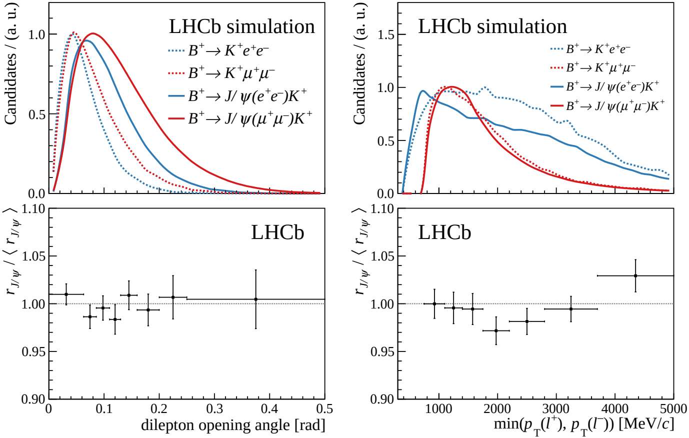

Cross-check 3: $r_{J/\psi}$ in 2D [PRL 122 (2019) 191801]

- Repeat the exercise in 2D, to check against correlated effects.
- Choose q^2-dependent variables relevant for the detector response.
- Select $B^+ \to K^+ J/\psi(\ell^+\ell^-)$ events in bins of this 2D space and compute $r_{J/\psi}$ in each of them

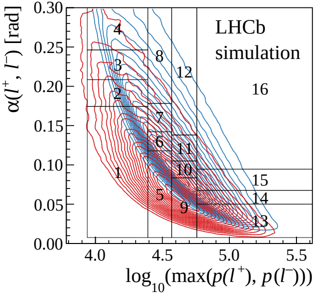

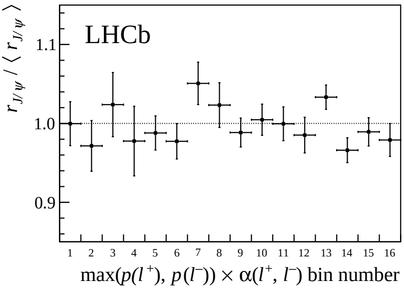

→ Flatness of $R^{2D}_{J/\psi}$ plots gives confidence that efficiencies are understood over all phase-space

Cross-check 4 & 5

[PRL 122 (2019) 191801]

- Measurement of the double ratio

$$R_{\psi(2S)} = \frac{\mathcal{B}(B^+ \to K^+\psi(2S)(\mu^+\mu^-))}{\mathcal{B}(B^+ \to K^+J/\psi(\mu^+\mu^-))} \Bigg/ \frac{\mathcal{B}(B^+ \to K^+\psi(2S)(e^+e^-))}{\mathcal{B}(B^+ \to K^+J/\psi(e^+e^-))},$$

Result well compatible with unity:

$$R_{\psi(2S)} = 0.986 \pm 0.013\,(\mathrm{stat} + \mathrm{syst})$$

$\rightarrow$ Good compatibility found separately for Run 1 and Run 2 datasets, and in all trigger categories.

- Checked that the $\mathcal{B}(B^+ \to K^+\mu^+\mu^-)$ is compatible with previous determination [LHCb JHEP06 (2014) 133], but less precise owing to the selection being optimised for R_K.

$\rightarrow$ Good compatibility between the measurements in the Run 1 and Run 2 samples is also found.

Systematics uncertainties

- Efficiency calibration
  - $\rightarrow$ Dependence with tag, in tag-and-probe determinations;
  - $\rightarrow$ Parameterisation bias (e.g. factorisation of PID efficiencies for kaons and electrons) tag and trigger bias;
  - $\rightarrow$ Dependence of q^2 and $m(K^+e^+e^-)$ resolution with q^2
  - $\rightarrow$ Inaccuracies in material description in simulation (tracking efficiency)
- Statistics of simulation and calibration samples
  - Bootstrapping method that takes into account correlations between calibration samples and final measurement
- Choice of fit model
  - Associated signal and partially reconstructed background shape

$\rightarrow$ Total relative systematic of 1.7% in the final R_K measurement $\Rightarrow$ Expected to be statistically dominated

Fit to the resonant modes

[PRL 122 (2019) 191801]

Yields for $B^+ \to K^+ J/\psi(\ell^+\ell^-)$, used as input for cross-checks and final determination of R_K, obtained from a fit to the J/ψ-constrained B mass

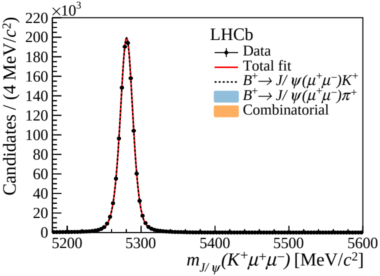

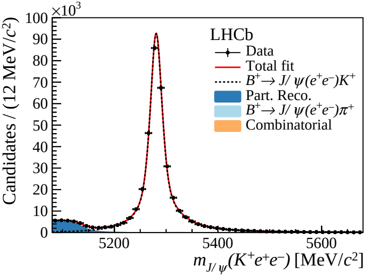

- Signal and background shapes determined from calibrated simulation
- Allow for a shift in the position in the signal peak and a scale factor to the resolution to float in the fit

Simultaneous fit to extract R_K

- Get R_K directly as a parameter of the fit
- Perform simultaneous fit to $m(K^+e^+e^-)$ and $m(K^+\mu^+\mu^-)$ distributions

$$R_K = \frac{N^r_{K\mu\mu}}{N^{rt}_{Kee}} \cdot \frac{N^{rt}_{J/\psi ee}}{N^r_{J/\psi\mu\mu}} \cdot \frac{\varepsilon^{rt}_{Kee}}{\varepsilon^r_{K\mu\mu}} \cdot \frac{\varepsilon^r_{J/\psi\mu\mu}}{\varepsilon^{rt}_{J/\psi ee}}$$

$$= \frac{N^r_{K\mu\mu}}{N^{rt}_{Kee}} \cdot c^{rt}_K,$$

for $r =$Run 1, Run 2 and $t =$L0Electron, L0Hadron, L0TIS.

- c^{rt}_K are included as a multidimensional Gaussian constraint, with uncertainties and correlations according to the 6×6 covariance matrix σ
- Partially reconstructed background comes essentially from $B \to K^* e^+e^-$ and so it can be constrained using

$$\frac{N^{r,t}_{prc}}{N^{r,\mathrm{eTOS}}_{prc}} = \frac{\varepsilon^{r,t}_{trig,mass}(K^*ee)}{\varepsilon^{r,\mathrm{eTOS}}_{trig,mass}(K^*ee)} = r^{rt}_{prc}$$

Fit to $B^+ \to K^+\ell^+\ell^-$ candidates

[PRL 122 (2019) 191801]

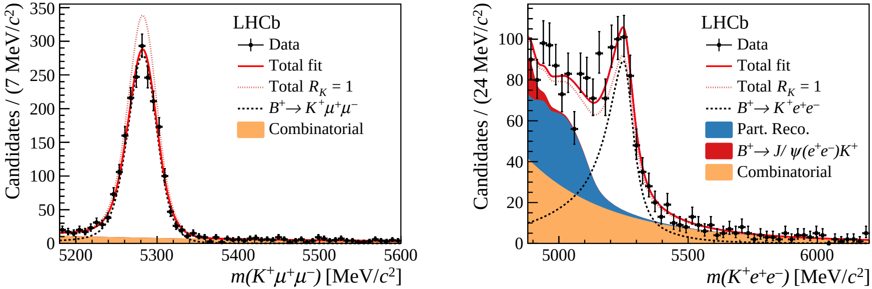

- Signal and background shapes determined from calibrated simulation.
- Mass shift and resolution scale fixed to that observed in the fit to the resonant mode.
- Leakage from $B^+ \to J/\psi(ee)K^+$ in the $B^+ \to K^+e^+e^-$ signal region ($1.1 < q^2 < 6.0\,\mathrm{GeV}^2/c^4$), constrained from the fit to the resonant mode.

Final results

[LHCb, PRL 113 (2014) 151601]

[BaBar, PRD 86 (2012) 032012]

[Belle, PRL 103 (2009) 171801]

* LHCb Run1 bin centre horizontally displaced for illustration.

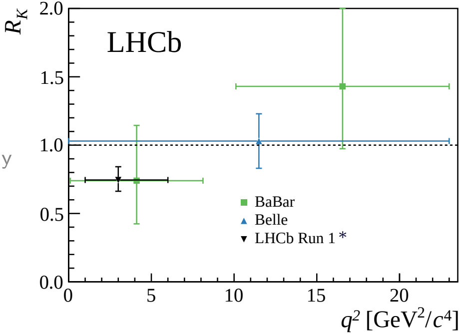

Using 2011 and 2012 LHCb data:

$$R_K = 0.745 \,^{+0.090}_{-0.074}\,(\text{stat}) \,\pm 0.036\,(\text{syst}),$$

compatible with the SM expectation at 2.6σ.

Final results

[PRL 122 (2019) 191801]

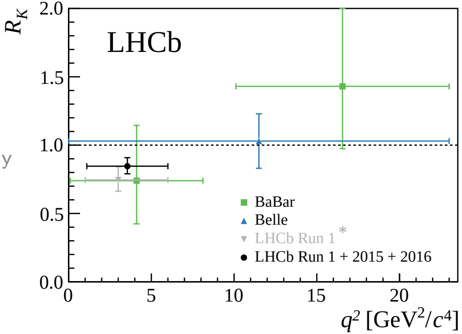

[LHCb, PRL 113 (2014) 151601]

[BaBar, PRD 86 (2012) 032012]

[Belle, PRL 103 (2009) 171801]

* LHCb Run1 bin centre horizontally displaced for illustration.

Using 2011 and 2012 LHCb data:

$$R_K = 0.745\,^{+0.090}_{-0.074}\,(\text{stat})\ \pm 0.036\,(\text{syst}),$$

compatible with the SM expectation at 2.6σ.

Reanalysing 2011-2012 and adding 2015 and 2016 data, R_K becomes

$$R_K = 0.846\,^{+0.060}_{-0.054}\,(\text{stat})\,^{+0.014}_{-0.016}\,(\text{syst})$$

which is compatible with the SM expectation at 2.5σ.

Final results (II)

[PRL 122 (2019) 191801]

- R_K is obtained from a simultaneous fit to Run 1 and Run 2 datasets.
- If instead the Run 1 and Run 2 were fitted separately:

$$R_K{}^{\text{old Run1}} = 0.745\,^{+0.090}_{-0.074}\,\pm 0.036\,,$$

$$R_K{}^{\text{new Run1}} = 0.717\,^{+\,0.083}_{-\,0.071}\,^{+\,0.017}_{-\,0.016}\,,$$

$$R_K{}^{2015\,+\,2016} = 0.928\,^{+\,0.089}_{-\,0.076}\,^{+\,0.020}_{-\,0.017}\,.$$

Compatibility taking correlations into account:

$\rightarrow$ Previous Run 1 result vs. this Run 1 result: $< 1\sigma$
(new reconstruction, selection)

$\rightarrow$ Run 1 result vs. Run 2 result: 1.9σ

Final results (III)

[PRL 122 (2019) 191801]

- Determination of $B^+ \to K^+\mu^+\mu^-$ branching fraction:
  - Compatible with previous result ([JHEP06(2014)133]),
  - Run 1 and Run 2 results also compatible,

- Combining the measurement of R_K with the previously published value for $\mathcal{B}(B^+ \to K^+\mu^+\mu^-)$ [LHCb-PAPER-2014-006]

$$\frac{\mathrm{d}\mathcal{B}(B^+\to K^+e^+e^-)}{\mathrm{d}q^2} = (28.6\ ^{+2.0}_{-1.7}(\mathrm{stat})\ \pm 1.4(\mathrm{syst})) \times 10^{-9}\ c^4/\,\mathrm{GeV}^2$$

in the range $q^2 \in [1.1, 6]\,\mathrm{GeV}^2/c^4$.

$\rightarrow$ Dominant systematic come from the $\mathcal{B}(B^+ \to K^+ J/\psi)$.

$\rightarrow$ This is the most precise determination of this branching fraction to date.

Impact on Global Fits

David M. Straub, Moriond EW 2019

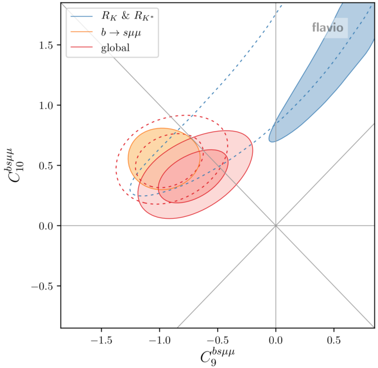

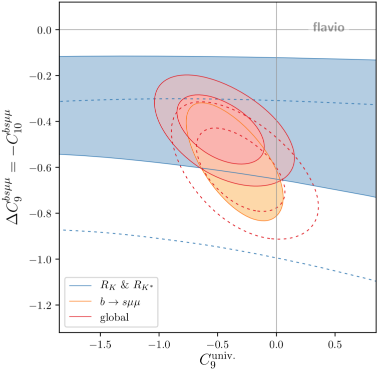

→ Best fit point still in tension with the SM

→ Worse compatibility between $R_K^{(*)}$ & $b \to s\mu^+\mu^-$ observables

→ Muonic NP: Best fit closer to the SM, $C_9 = -C_{10}$ still preferred

→ Adding LFU NP: Slight preference for universal shift in C_9

[M. Algueró et al., arXiv:1903.09578, A. K. Alok et al., arXiv:1903.09617, M. Ciuchini et al., arXiv:1903.09632, Guido D'Amico et al., arXiv:1704.05438, A. Data et al., arXiv:1903.10086, J. Aebischer et al., arXiv:1903.10434, A. Crivellin et al., arXiv:1903.10440]

Prospects on LFU tests

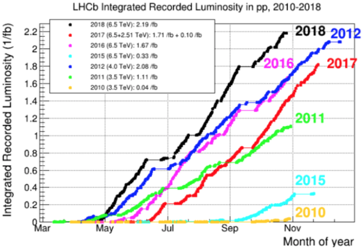

- LHCb full Run 2 dataset ~ 4 times number of B's available in Run1
  - Updates of R_K and $R_{K^{*0}}$, and many other LFU ratios: R_ϕ, R_{pK}, R(D), $R(\Lambda_c)$…
  - Angular analysis of $b\to s\ell\ell$ transitions also underway
- CMS has collected a sample of 10^{10} B decays
  - With an effective low p_T electron reconstruction, should get a very competitive number of e.g. $B^+\to K^+e^+e^-$ signal candidates
  - Expect systematics will be very different to those at LHCb e.g. no trigger effect and very different material distribution
- ATLAS pursuing a similar strategy
- Belle II starting data-taking this year

Further into the future [CERN-LHCC-2011-001]

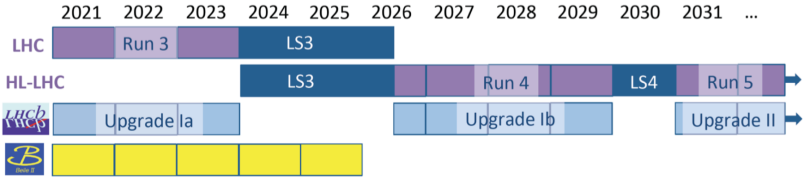

- LHCb is in the process of upgrading to a new detector
  - will operate at much higher luminosity with improved efficiency (make all trigger decisions in software)
  - will accumulate 50 fb^{-1} of data
- A second phase of the Upgrade in LS4 is also planned to profit from even higher luminosities at the HL-LHC (increase data sample up to 300 fb^{-1} for LHCb)

LFU with upgrade datasets

[LHCb-PUB-2018-009]

- Access to different LFU ratios with excellent precision: allow to distinguish between different NP scenarios
  - Need to drive systematics in electrons down to ~ 1%
- LFU tests with angular observables
  - e.g. $Q_5 = P'_5(\mu) - P'_5(e)$

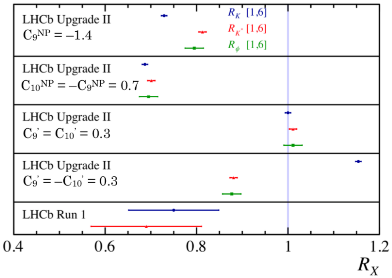

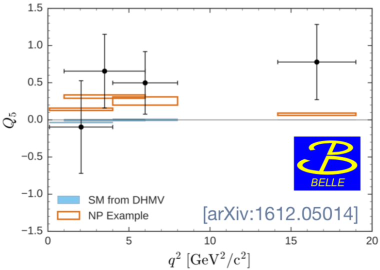

Conclusions

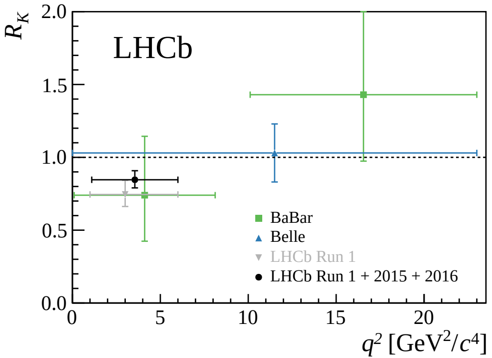

- Lepton Flavour Universality tests are theoretically pristine probes for New Physics.
- Latest measurements yet to provide a definitive picture.
- Upcoming measurements with full Run 2 statistics will help to resolve the current situation.

BACKUP

What type of NP would $C_9^{NP} = -1.5$ correspond to?

- NP contributions enter into Lagrangian as

$$\mathcal{L}_{NP} = \frac{c_{NP}}{\Lambda_{NP}^2}\mathcal{O}_{NP}$$

- Lack of evidence for New Physics in flavour observables $\Rightarrow \Lambda_{NP}$ is large or couplings, c_{NP}, are small (e.g. MFV)

- Translating C_9^{NP} into c_{NP} & Λ_{NP}:

	c_{NP}	Λ_{NP}
tree-level	$\mathcal{O}(1)$	35 TeV
tree-level	MFV	7 TeV
loop	$\mathcal{O}(1)$	2.8 TeV
loop	MFV	0.6 TeV

LFU in Charged Currents: $b \to c\ell\nu$

- Very clean observables in the SM

$$R(D^*) = \frac{\mathcal{B}(B^0 \to D^{*-}\tau^+\nu_\tau)}{\mathcal{B}(B^0 \to D^{*-}\mu^+\nu_\mu)} \stackrel{SM}{=} 0.258 \pm 0.005$$

[HFLAV average]

- Challenging for LHCb due to the presence of multiple neutrinos
- Two LHCb measurements in Run1 (2011+2012) using different reconstructions of the τ decay
  - $\tau \to \mu\nu\nu$ [LHCb, PRL 115 (2015) 111803]
  - $\tau \to 3\pi(\pi^0)\nu$: [LHCb, PRL 120 (2018) 171802] [LHCb, PRD 97 (2018) 072013]

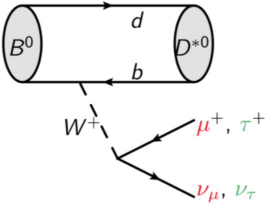

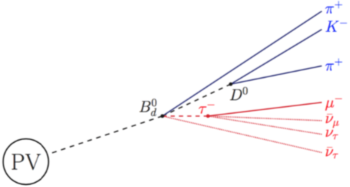

$R(D)$ and $R(D^*)$ combination

[BaBar, PRL 109,101802 (2012)]
[LHCb, PRL 115 (2015) 111803]
[Belle, PRD 92 (2015) 072014]
[Belle, PRL 118 (2017) 211801]
[LHCb, PRL 120 (2018) 171802]
[Belle, arXiv:1904.08794v2 (2019)]

Combining with results from the B-factories:

→ Global tension with the SM prediction of **3.08σ**

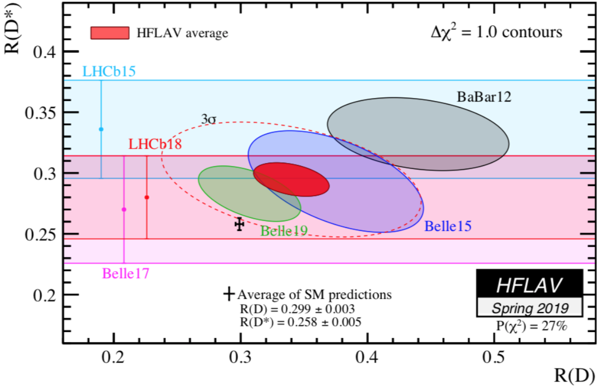

Link to Lepton Flavour Violation

- Attempts to explain tensions in FCCC and FCNC simultaneously, usually point to enhancements in LFV processes ($B \to \ell\ell'$, $B \to K\ell\ell'$,…)
  - e.g. vector lepto-quark contributing at tree-level to R(D*) and at loop-level to R_K

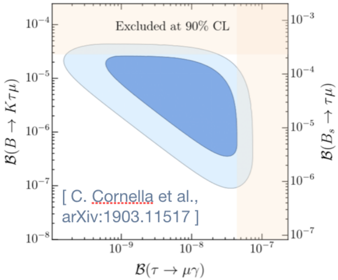

- New searches for $B_{(s)} \to \tau\mu$ with LHCb Run1 data

Mode	Limit	90% CL	95% CL
$B_s^0 \to \tau^\pm\mu^\mp$	Observed	3.4×10^{-5}	4.2×10^{-5}
	Expected	3.9×10^{-5}	4.7×10^{-5}
$B^0 \to \tau^\pm\mu^\mp$	Observed	1.2×10^{-5}	1.4×10^{-5}
	Expected	1.6×10^{-5}	1.9×10^{-5}

First limit in the Bs mode

[LHCb-PAPER-2019-016]

Cross-check 3: $r_{J/\psi}$ in 2D

- Our control channel sits at $q^2 = (m_{J/\psi})^2$, however the detector response is not a direct function of q^2...
- ... rather it depends on different set of variables that are a function of q^2: $\alpha_{J/\psi}$, $\max p_\ell$, $\min p_\ell$, α_ℓ, $(\alpha_{B+}, \phi_B, \phi_{\ell\ell}, \phi_\ell)$

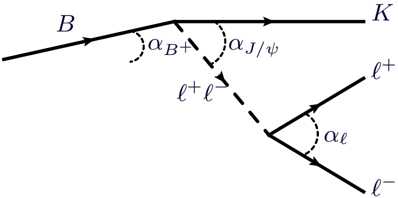

- In these variables, $B^+ \to K^+ J/\psi(e^+e^-)$ decays give good coverage of the rare decay spectrum in 1D and even 2D.

$\rightarrow$ Parameterise the decay in the frame of the detector and use the high yield of the J/ψ mode to look for trends as a function of these variables.

Fit window for $B^+ \to K^+ e^+ e^-$ [PRL 122 (2019) 191801]

Remaining backgrounds:

- Combinatorial
- $B^+ \to K^+ J/\psi(e^+e^-)$
- Partially reconstructed $B \to K X \ell\ell$ decays

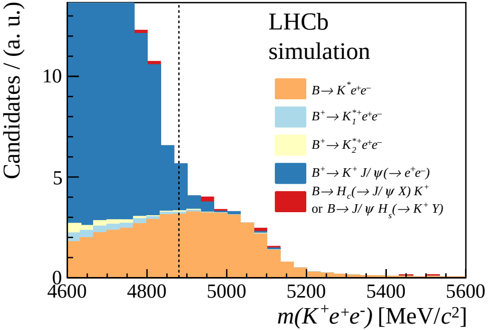

Choose the $m(K^+e^+e^-)$ window so that the contribution from partially reconstructed decays is dominated by $B^0 \to K^{*0}e^+e^-$,

$\to$ Included the contribution from $B \to K^{**}e^+e^-$ decays, $K^{**} \equiv \{K_1, K_2^{*0(+)}\}$, as a systematic

$$\mathcal{B}(B \to K^{**}e^-e^-) = \mathcal{B}(B^0 \to K^{*0}e^-e^-) \cdot \mathcal{B}(B \to K^{**}J/\psi)/\mathcal{B}(B^+ \to K^{*0}J/\psi)$$

Compatibility with the Standard Model

[PRL 122 (2019) 191801]

- Include a Gaussian constraint on the SM prediction for R_K, to take into account the theory uncertainty ($\mathcal{O}(10^{-2})$).
- Compatibility with the SM obtained by integrating the profiled likelihood as a function of R_K above 1
- The result is compatible with the SM at 2.5 standard deviations.

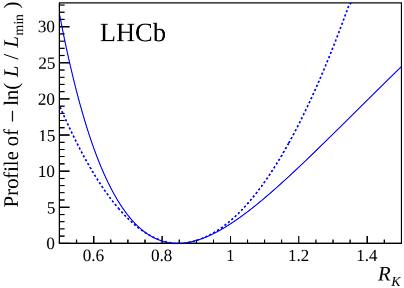

Solid line represents the profiled likelihood. For reference, dashed lines depict quadratic behaviour.

Compatibility between categories

- Checked compatibility with previous analysis [LHCb, PRL 113 (2014) 151601] taking into account the sample overlap
- Checked internal compatibility of the analysis - 3 trigger categories and 2 runs
  - Look at $\Delta \log \mathcal{L} = \min(\log \mathcal{L})_{\text{indep}} - \min(\log \mathcal{L})_{\text{comb}}$

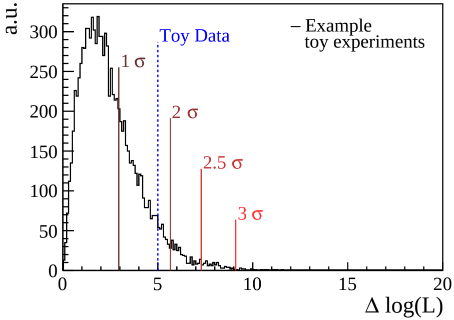

Effective Theory

- Model independent description in effective field theory

$$\mathcal{H}_{\text{eff}} = -\frac{4G_F}{\sqrt{2}} V_{\text{tb}} V_{\text{ts}}^{*} \frac{e^2}{16\pi^2} \sum_i \underbrace{\boxed{\mathcal{C}_i}}_{\text{Wilson coefficient ("effective coupling")}} \overbrace{\boxed{\mathcal{O}_i}}^{\text{Local operator}} \qquad \Delta\mathcal{H}_{\text{NP}} = \frac{\overbrace{\boxed{\kappa}}^{\text{Flavour-violating coupling}}}{\underbrace{\boxed{\Lambda^2_{\text{NP}}}}_{\text{NP scale}}} \mathcal{O}_i$$

- NP can contribute to different operators $\mathcal{O}_i$ depending on its type. Relevant effective couplings for rare decays:

		Coupling	Operator
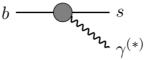	Photon penguin	$\mathcal{C}_7^{(\prime)}$	$\frac{m_b}{e}(\bar{s}\sigma_{\mu\nu}P_{R(L)}b)F^{\mu\nu}$
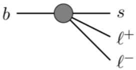	EW penguin	$\mathcal{C}_9^{(\prime)}$	$(\bar{s}\gamma_\mu P_{L(R)}b)(\bar{\mu}\gamma^\mu\mu)$
		$\mathcal{C}_{10}^{(\prime)}$	$(\bar{s}\gamma_\mu P_{L(R)}b)(\bar{\mu}\gamma^\mu\gamma_5\mu)$
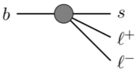	Scalar penguin	$\mathcal{C}_S^{(\prime)}$	$\frac{m_b}{m_B}(\bar{s}P_{R(L)}b)(\bar{\mu}\mu)$
		$\mathcal{C}_P^{(\prime)}$	$\frac{m_b}{m_B}(\bar{s}P_{R(L)}b)(\bar{\mu}\gamma_5\mu)$

$b \to s\gamma$ ($\mathcal{C}_7^{(\prime)}$)

$b \to s\ell\ell$ ($\mathcal{C}_7^{(\prime)}$, $\mathcal{C}_9^{(\prime)}$, $\mathcal{C}_{10}^{(\prime)}$)

$B_s^0 \to \mu^+\mu^-$ ($\mathcal{C}_{10}^{(\prime)}$, $\mathcal{C}_S^{(\prime)}$, $\mathcal{C}_P^{(\prime)}$)